

Research Article

The Applicability of Different Fluid Media to Measure Effective Stress Coefficient for Rock Permeability

Ying Wang,¹ Guozhi Li,¹ Min Li,¹ and Jing Zhang²

¹State Key Laboratory of Oil and Gas Geology and Exploitation, Southwest Petroleum University, Chengdu 610500, China

²Xinjiang Oilfield Company, China National Petroleum Corporation, Xinjiang 834000, China

Correspondence should be addressed to Min Li; hytlxf@126.com

Received 6 December 2014; Revised 28 February 2015; Accepted 28 February 2015

Academic Editor: Agus Sasmito

Copyright © 2015 Ying Wang et al. This is an open access article distributed under the Creative Commons Attribution License, which permits unrestricted use, distribution, and reproduction in any medium, provided the original work is properly cited.

Effective stress coefficient for permeability (ESCK) is the key parameter to evaluate the properties of reservoir stress sensitivity. So far, little studies have clarified which ESCK is correct for a certain reservoir while rock ESCK is measured differently by different fluid media. Thus, three different fluids were taken to measure a fine sandstone sample's ESCK, respectively. As a result, the ESCK was measured to be the smallest by injecting nitrogen, the largest by injecting water, and between the two by brine. Besides, those microcharacteristics such as rock component, clay mineral content, and pore structure were further analyzed based on some microscopic experiments. Rock elastic modulus was reduced when water-sensitive clay minerals were encountered with aqua fluid media so as to enlarge the rock ESCK value. Moreover, some clay minerals reacting with water can spall and possibly block pore throats. Compared with water, brine can soften the water sensitivity; however, gas has no water sensitivity effects. Therefore, to choose which fluid medium to measure reservoir ESCK is mainly depending on its own exploitation conditions. For gas reservoirs using gas to measure ESCK is more reliable than water or brine, while using brine is more appropriate for oil reservoirs.

1. Introduction

The characteristics of reservoir stress sensibility for rock permeability mainly behave as follows: with the on-going exploitation of oil and gas, the pore pressure of reservoir is decreasing, while the effective stress is increasing. As a result, the pore volume of reservoir is reducing and the reservoir permeability is lowering. To reasonably evaluate the reservoir effective stress sensitivity for permeability has a major impact on analyzing productivity, adjusting proration, and scheduling recovery. Meanwhile, it can help to recognize the reservoir permeability varying rules and mechanisms [1]. Reservoir effective stress sensitivity for permeability is characterized as ESCK. As early as 1923 [2], Terzaghi firstly mentioned the effective stress sensitivity for soil permeability. After that, a large number of studies were emphasized on measuring ESCK by using various kinds of fluid media, including nitrogen, water, and brine.

Some studies, conducted by Warpinski and Teufel [3], Li and Xiao [1], and others, based on using nitrogen as the fluid medium, show that the ESCK of low permeable

sandstone with clay is between 0.8 and 1.06, those with illite-montmorillonite mixed-layer are between 0.55 and 1.1, and those with chlorite-montmorillonite mixed-layer are between 0 and 1.12. Furthermore, the rock ESCK is reducing with the confining pressure increasing while increasing with the pore pressure increasing.

Other studies, conducted by Nur et al. [4], Morrow et al. [5], Bernabe [6], and others, on the basis of using distilled water as the fluid medium, show that the ESCK value of sandstone containing 0.5~8.6% kaolinite is between 1.2 and 4.6, those containing 20% kaolinite are 7.1, those for Westerly granite are between 0.95 and 1.23, those for Barre granite are between 0.43 and 1.1, those for low permeability sandstone are 1.3 and 3.1, and those for Pottsville sandstone, Pigeon Cove granite are close to 1.0. In addition, the more the clay minerals content is in rock, the larger the rock ESCK is.

And some studies, conducted by Coyner [7], Kwon et al. [8], Nur et al. [4], Al-Wardy and Zimmerman [9], Boitnott et al. [10], and others, in accordance with using brine as the fluid medium show that the ESCK value of Berea sandstone is larger than 1, those for shale containing

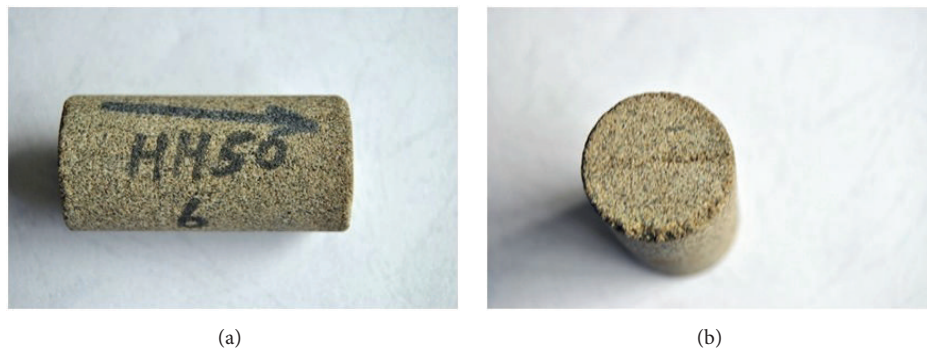


FIGURE 1: Photos of the sample appearance.

40%–50% illite are quite equal to 1.0, and those for Berea sandstone containing 6%, 4.3%, and 8% kaolinite are 2.9, 3.2, and 5.4, respectively. Moreover, the ESCK values of sandstone with clay under three different loading sequences in their studies were different, 2.0, 2.4, and 2.8, respectively.

Moreover, there are some other studies measuring the ESCK value by using oil. In addition, Zoback and Byerlee [11] tested Berea sandstone (containing 8% clay) ESCK, 2.2, by using lubricating oil as the fluid medium. Kranzz et al. [12] tested Berea granite ESCK, less than 1, by using kerosene. Nur et al. [4] tested the ESCK values for sandstone with 8% and 6% kaolinite to be 4 and 3.5, respectively.

According to previous studies, reservoir ESCK value is affected by multifactors such as fluid media, rock components, clay content and its distribution, mineral composition, and pore structure. The ESCK value measured by nitrogen is usually less than 1, increasing with clay mineral content increasing. The ESCK value measured by distilled water is close to 1 for granite while it is larger than 1 for sandstone and is also increasing with clay mineral content increasing up to 7.1. The ESCK value measured by brine is usually greater than 1 and between that of nitrogen and distilled water. Though many scholars adopted different fluid media to measure out different ESCK values in different range for different rock samples, no one used different fluid media to measure the same sample and discuss the difference on ESCK. A series of ESCK measurement experiments by using three different fluid media (e.g., 99.99% nitrogen, distilled water, and brine with 50000 ppm potassium chloride, KCl) to flow through a fine sandstone sample were conducted in this study. As a result, under the same condition, the value of ESCK for the same sample is smallest by injecting nitrogen, largest by injecting distilled water, and between both by injecting brine. Hence, the microscopic characteristics of the tested sample, such as mineral composition, clay content, and pore structure, were further analyzed by conducting some related microscopic experiments. The fact that the ESCK for the same rock sample is measured to be different by using different fluid media is directly dependent on the microscopic characteristics of rock. Finally, the behaviors of fluid media with rock ESCK were discussed in this study.

2. Experimental Setup and Method

2.1. Fluid Media and Properties. In order to study the influences of different media on rock ESCK and the reliability of ESCK measurement, three different fluid media, 99.99% nitrogen, distilled water, and brine with 50000 ppm KCl, were used to measure the ESCK of a fine sandstone sample.

2.2. Rock Sample and Microscopic Characteristics. The sandstone sample studied in this paper was drilled from a representative Chinese reservoir. And the photos of the sample appearance are shown in Figures 1(a) and 1(b). The fundamental properties of this sample (labeled HH50-06) including porosity, permeability, density, and clay content were tested by conventional methods (shown in Table 1). Besides, the microscopic characteristics of this sample were measured by several microscopic methods such as cast thin section, SEM, X-ray diffraction, and Mercury Injection. The SEM images of this sample at different magnification times are shown in Figures 2(a)~2(e). The cast thin section image of this sample is shown in Figure 3. The results of Mercury Injection tests of this sample are shown in Figures 4(a) and 4(b).

Microscopic characteristics of this sample are described as follows.

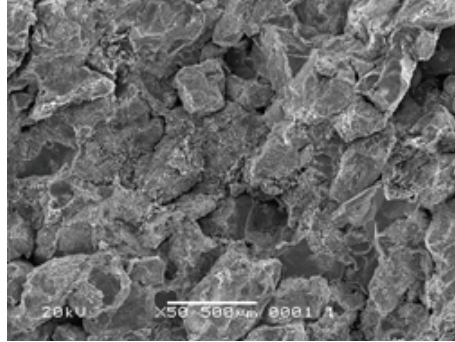
(i) According to SEM tests and the images (shown in Figure 2), the sample has loose structure, clear outline of detrital particles, quartz secondary enlargement, developed intergranular pores, and fractures (shown in Figure 2(a)). Besides, schistose illites adhere to the surfaces of granules, secondary quartz crystals. And calcite crystals fill in part of the intergranular pores (shown in Figures 2(b)~2(d)). Booklet kaolinite bundles fill in part of the intergranular pores and kaolinite bundles are mixed with some schistose illites. And some feldspar particles are corroded to be secondary corrosion pores (shown in Figure 2(e)).

(ii) According to X-ray diffraction tests, most of the clay minerals are kaolinite and chlorite; next is illite-smectite interlayer, content of which is 19.6% and content ratio of which is 16%.

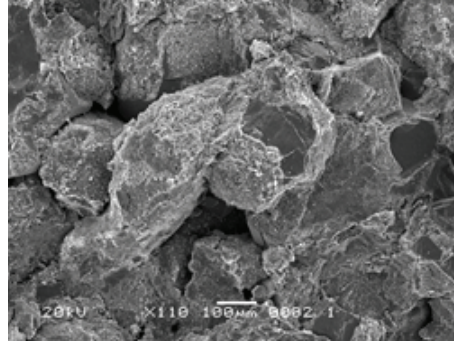
(iii) According to Mercury Injection tests and the images (shown in Figure 4), the capillary force curve of the sample is inclined, and pore-throat sizes are poor sorting. Pore spaces are the main reservoir spaces of this rock.

TABLE 1: Fundamental properties of this sandstone sample.

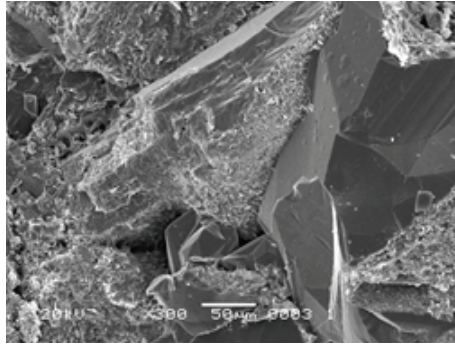
Porosity (%)	Permeability (mD)	Depth (m)	Density (g/cm ³)	Clay (%)	Length (cm)	Diameter (cm)
11.30 ± 1.56	0.53 ± 0.19	2428.01 ± 56.04	2.4 ± 0.11	11 ± 2.32	5.03 ± 0.44	2.47 ± 0.02



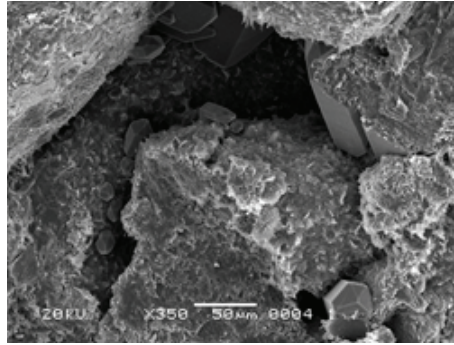
(a) 50 times



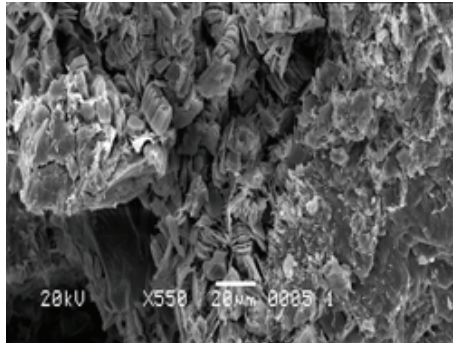
(b) 110 times



(c) 300 times



(d) 350 times



(e) 550 times

FIGURE 2: SEM images of this sample at different magnification times.

(iv) According to cast thin section tests and the image (shown in Figure 3), cemented type of the sample is porous cementation, contacted type is spot-line contact, and rock granule performs well in sorting and with subangular edge. Besides, rock debris takes quartz primarily and clay secondarily.

2.2.1. Sample Preparation. In this study, the ESCK of this sample HH50-06 was firstly measured by nitrogen, then by distilled water, and finally by brine, respectively. To measure rock ESCK by a fluid medium such as nitrogen, the sample was dried over 24 hours in an oven and kept in a desiccator.

After that, the sample was placed in the core holder, vacuumed for over two hours, and saturated with nitrogen under pressure for over eight hours. When measured by distilled water or brine, it was the same to prepare sample like the above.

2.3. Experimental Theory and Method

2.3.1. ESCK Measurement Theory. Based on the conception of effective stress, the effective stress of permeability can be expressed as follows:

$$k = f(P_c, P_p) = f(P_{\text{eff}}) = f(P_c - \kappa P_p), \quad (1)$$

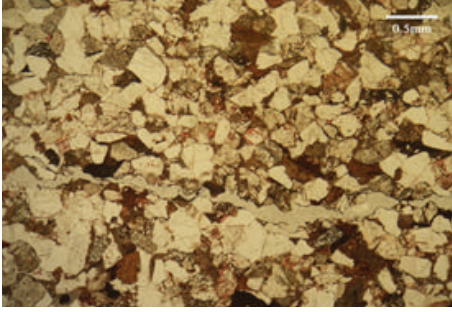


FIGURE 3: Cast thin section image of this sample.

$$\kappa = -\frac{\partial k / \partial P_p}{\partial k / \partial P_c} = -\frac{\delta k_p}{\delta k_c}, \quad (2)$$

$$\kappa = -\frac{\partial k / \partial P_p}{\partial k / \partial P_c} = -\frac{a_3 + a_5 P_c + 2a_6 P_p}{a_2 + 2a_4 P_c + a_5 P_p}, \quad (3)$$

where k is effective stress coefficient for permeability (ESCK), which means the ratio of confining pressure variation and pore pressure variation when permeability is constant. Response surface method is adopted to calculate ESCK in this study.

And the steps to calculate ESCK are as follows.

- (1) Transform the tested permeability data into a simple form so as to minimize the sum of squared residuals.
- (2) Match the transformed permeability data by quadric surface or linear plane to be the best.
- (3) Combined with regression coefficient, calculate ESCK at different confining pressure P_c and pore pressure P_p .

2.3.2. The Principals of Transient Pulse Decay Permeability Measurement. The pressure diffusion across the sample can be expressed as follows [13]:

$$\frac{\partial^2 p}{\partial x^2} = \left[\frac{\mu}{k} \phi \left(C_f + \frac{C_{\text{eff}}}{\phi} - \frac{1 + \phi}{\phi} C_s \right) \right] \frac{\partial P}{\partial t} \quad (4)$$

$$t > 0, \quad 0 < x < L.$$

Initial conditions are as follows:

$$\begin{aligned} P_1(0, 0) &= P_i, \quad t = 0, \quad x = 0, \\ P_R(x, 0) &= P_0, \quad t = 0, \quad 0 < x < L, \\ P_2(L, 0) &= P_0, \quad t = 0, \quad x = L. \end{aligned} \quad (5)$$

Boundary conditions are as follows:

$$\begin{aligned} \frac{\partial P}{\partial x} &= \frac{\mu V_1 C_f}{AK} \frac{\partial P}{\partial t}, \quad t > 0, \quad x = 0, \\ \frac{\partial P}{\partial x} &= -\frac{\mu V_2 C_f}{AK} \frac{\partial P}{\partial t}, \quad t > 0, \quad x = L. \end{aligned} \quad (6)$$

The equations to calculate gas and liquid are as follows [13]:

$$\begin{aligned} k_g &= \frac{-101.35m\mu_g L f_z}{f_1 A p_m (1/V_1 + 1/V_2)}, \\ k_l &= \frac{-101.35m\mu_l L (c_l + c_{v1})}{f_1 A (1/V_1 + 1/V_2)}, \end{aligned} \quad (7)$$

where k_g and k_l are the gas and liquid permeability, mD; m is the slope of linear equation, s^{-1} ; μ_g and μ_l are the viscosity of gas and liquid, mPa-s; f_z is compressibility correction factor, dimensionless; f_1 is mass flow correction factor, dimensionless; L is the length of sample, cm; A is the cross-sectional area of sample, cm^2 ; p_m is the mean absolute pore pressure, MPa; V_1 and V_2 are the volume in upstream and downstream reservoir, cm^3 .

2.4. Experimental Setup and Procedures

2.4.1. Experimental Setup. Rock permeability was measured by using transient pulse decay method, which was proposed by Brace et al. [14] as early as 1968. The ESCK measurement experiments were conducted on the home-made setup, which is shown in Figure 5. Rock sample was put in core holder (316L SS), one side of which was connected to upstream reservoir (V_1 , 316L SS) and the other side was connected to downstream reservoir (V_2 , 316L SS). The upstream reservoir was connected to a syringe pump (ISCO 100 D) which filled with high pressure fluid media (e.g., nitrogen, distilled water, and brine). The downstream reservoir was connected to vacuum pump. Besides, the confining pump (ISCO 100 D) filling with high pressure water was connected to the side of core holder. A differential pressure transducer (Validyne DPI5) and a communication valve (Valve 2, Swagelok) were connected to both sides of core holder, respectively. When the entire system was kept in a certain temperature and pressure to be stable, close Valve 2, and then a transient pulse produced by gas syringe pump went through the upstream reservoir, rock sample to the downstream reservoir. Then the differential pressure between the upstream and downstream reservoirs could be observed and recorded by a DAQ card (NI USB6008) to calculate the sample permeability in accordance with the above theories.

2.4.2. Experimental Procedures. Firstly, start the ESCK measurement with nitrogen. At the beginning, aging tests were treated to the sample in order to make its physical properties more stable.

Aging Tests. In consideration of the depth and density of the rock sample strata, the aging tests were operated as follows. (i) Load fluid pressure (i.e., pore pressure P_p) 1MPa and keep pore pressure constant. Load confining pressure from 5 to 50 MPa step by step with 5 MPa increase and keep each confining pressure stable. At each confining pressure P_c , a transient pulse pressure of 0.5 MPa was triggered by syringe pump and a pulse decay curve was real-time recorded to calculate the permeability k . (ii) Unload confining pressure

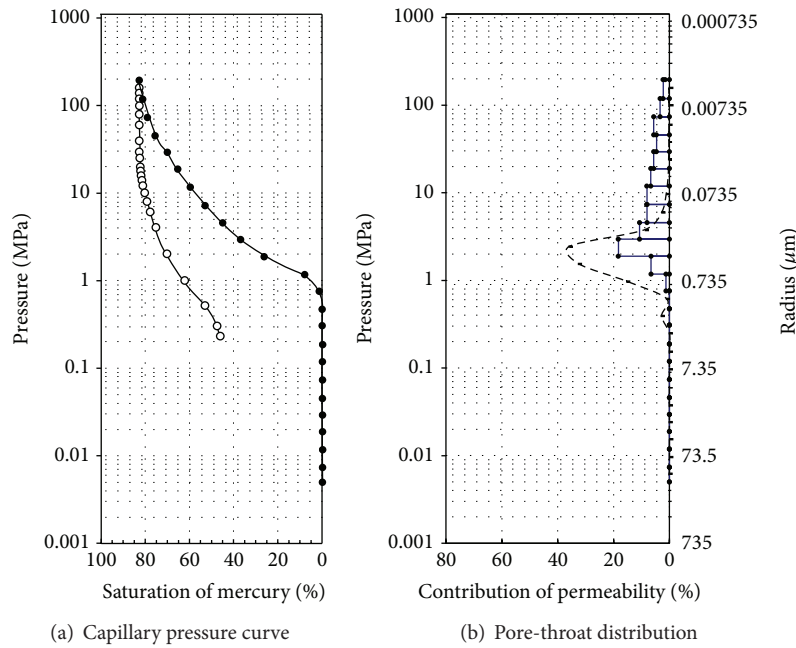


FIGURE 4: Results of Mercury Injection tests of this sample.

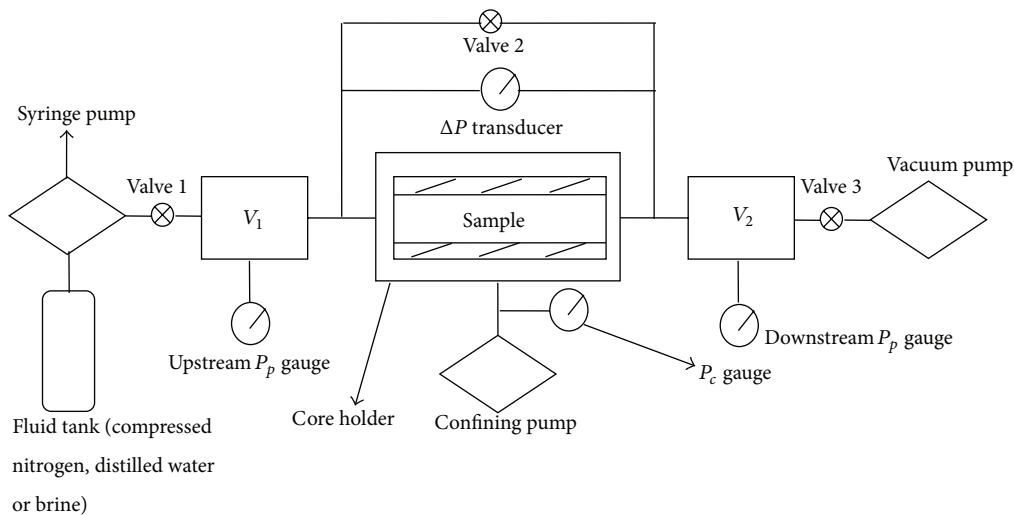


FIGURE 5: Sketch of the experimental setup.

from 50 to 5 MPa step by step with 5 MPa decrease and keep each confining pressure stable. Permeability k was also measured and calculated at each confining pressure P_c . (iii) Repeat the above loading/unloading confining pressure cycles twice.

ESCK Tests. After aging tests, continue the ESCK measurement for the sample. At the beginning, load confining pressure up to 50 MPa and pore pressure to 25 MPa, and keep the entire system equilibrated over 12 hours. Next, specific experimental procedures were as follows.

Step 1. At confining pressure of 50 MPa, unload pore pressure from 25 to 5 MPa step by step with 5 MPa decrease and keep system stable over 30 min at each pore pressure. Meanwhile,

sample permeability was measured and calculated at each pore pressure. Then load pore pressure from 5 to 25 MPa step by step with 5 MPa increase and proceed to the next procedures as the above unloading scenario.

Step 2. After Step 1, unload confining pressure from 50 to 40 MPa and keep entire system equilibrated over 30 min. Then do the pore pressure loading/unloading cyclic procedures like Step 1.

Step 3. After Step 2, unload confining pressure from 40 to 30 MPa and also keep system stable over 30 min. Then do the pore pressure loading/unloading cyclic procedures like Step 1 or Step 2, too.

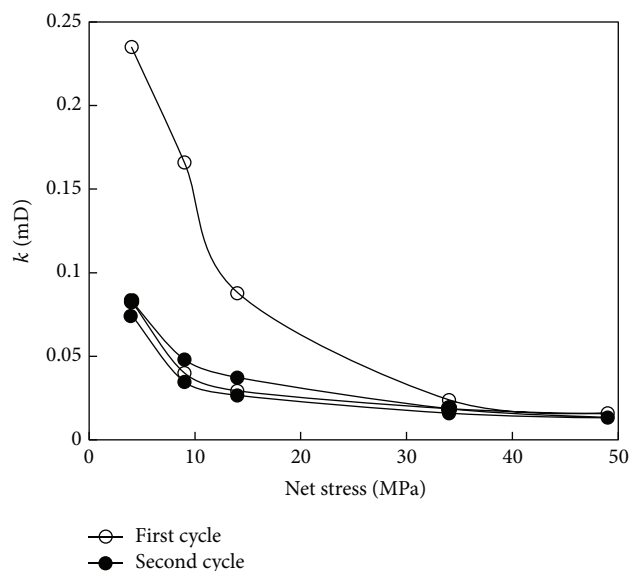


FIGURE 6: Permeability versus net stress in aging tests.

All of the permeability measurements for aging tests and ESCK tests were carried out in three repetitions.

3. Results and Analyses

3.1. Results and Analyses for Ageing Tests. The relationship between permeability and net stress, which means the difference of confining pressure and pore pressure, in accordance with aging tests is shown in Figure 6.

(1) With the increase of net stress, permeability firstly drops sharply and then decreases gradually at the first loading cycle, because in the early time of loading confining pressure, the initial existing microcracks are closing so as to narrow the flowing channels. Meanwhile, the permeability is reducing. In the late time of loading confining pressure, the pore spaces start to reduce until they are unchangeable indicating that larger confining pressure no longer induces any deformation of pore throats or pore bodies. As a result, the permeability is also a constant. Rock deformation turns from plastic into elastic stage.

(2) At the first unloading cycle with the net stress reducing, permeability is raising up to recover but less than the value of initial state. It is called lag effects of permeability. According to the microscopic characteristics of the sample, lag effects are primarily due to the clay minerals and other matters which are preferred to deform plastically after loading net stress. Besides, those deforming matters are easily blocking pore throat and hindering the permeability permanently. In addition, the inner surfaces of closed microcracks might be broken and be rubbing and sliding. It also possibly lowers the permeability.

(3) At the second cycle of loading/unloading net stress, rock sample performs elastic deformation and its permeability is recoverable. Permeability variations of the sample become stable. Plastic deformation disappears and tests can be repeated.

(4) At the first cycle, load the confining pressure up to 50 MPa, the permeability reduces totally 93.19%. In the stage when the confining pressure is larger than 20 MPa, the permeability varies a little. It is implied that the sample physical properties such as permeability and its microscopic characteristics are tending towards stability after one aging cycle.

3.2. Results and Analyses for ESCK Measurement. The relationships among permeability, confining pressure, and pore pressure for the sample when unloading and loading the pore pressure under nitrogen, distilled water, and brine are shown in Figures 7, 8, and 9, respectively. And those relationships of the sample under unloading and loading conditions of pore pressure are shown in (a) and (b) in each figure.

Comparing Figures 7(a) and 7(b), both illustrate that sample's permeability is decreasing in pore pressure unloading processes but rebounding well with the decreasing trend in the following pore pressure loading processes. When unloading or loading pore pressure under a low confining pressure (e.g., 30 MPa), the sample's permeability decreases or increases greatly.

From Figures 8(a) and 8(b), the permeability measured by distilled water decreases sharply. Comparing Figure 8 with Figure 7, the permeability measured by distilled water is generally lower and only 10% of the permeability measured by nitrogen under the same experimental conditions.

Comparing Figure 9 with Figure 8, the properties of the sample's permeability varying trend are close to those measured by distilled water. However, the sample's permeability is larger than that measured by distilled water and still lower than that measured by nitrogen.

From Figures 7~9, the sample's permeabilities measured by three different fluid media (nitrogen, distilled water, and brine) all perform the same changes. The permeability is increasing when pore pressure increases and decreasing when confining pressure increases. Under a low confining pressure condition, those permeabilities enlarge more obviously with pore pressure increasing. Under a high pore pressure condition, those permeabilities also reduce largely with confining pressure increasing. From Figures 8 and 9, the sample's permeabilities measured by aqua fluid media (distilled water and brine) display few changes with confining pressure changing.

3.3. Response Surface Method and ESCK Calculation. Based on response surface method, the measured ESCK data in this study can be calculated successfully. The related conversion factors (λ) and regression coefficients ($a_1 \sim a_6$) tested by nitrogen, distilled water, and brine are shown in Table 2.

After that, according to (3), the sample's ESCK values can be calculated and summarized in Table 3.

As a result, consider the following.

(1) When measured by nitrogen, the average ESCK value of the sample is 0.78 under pore pressure unloading conditions, while it is 0.54 under pore pressure loading conditions. It demonstrated that rock ESCK measurement is affected by the lag effects.

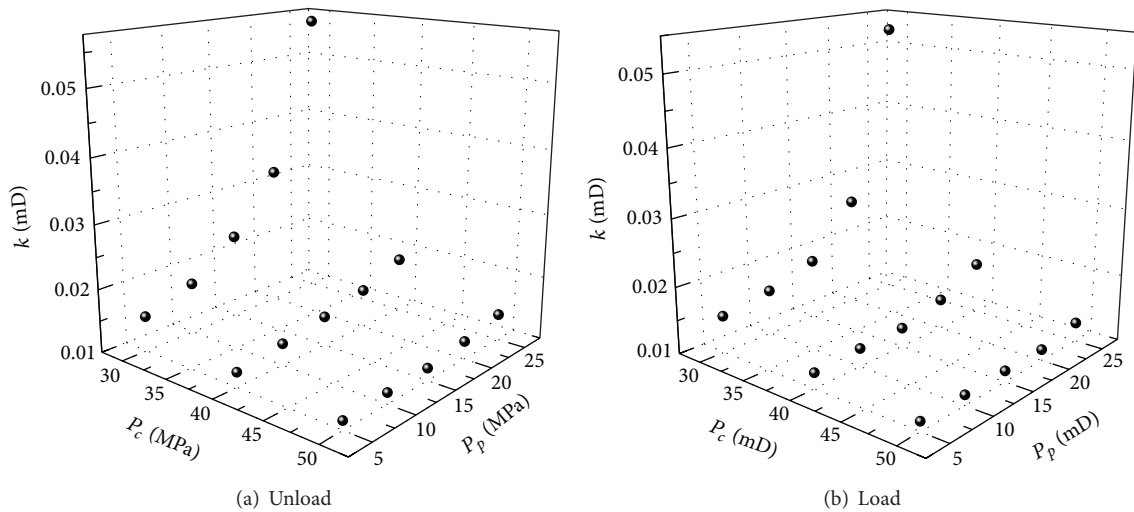


FIGURE 7: Permeability versus pore pressure and confining pressure measured by nitrogen when unloading (a)/loading (b) the pore pressure under three different confining pressure conditions.

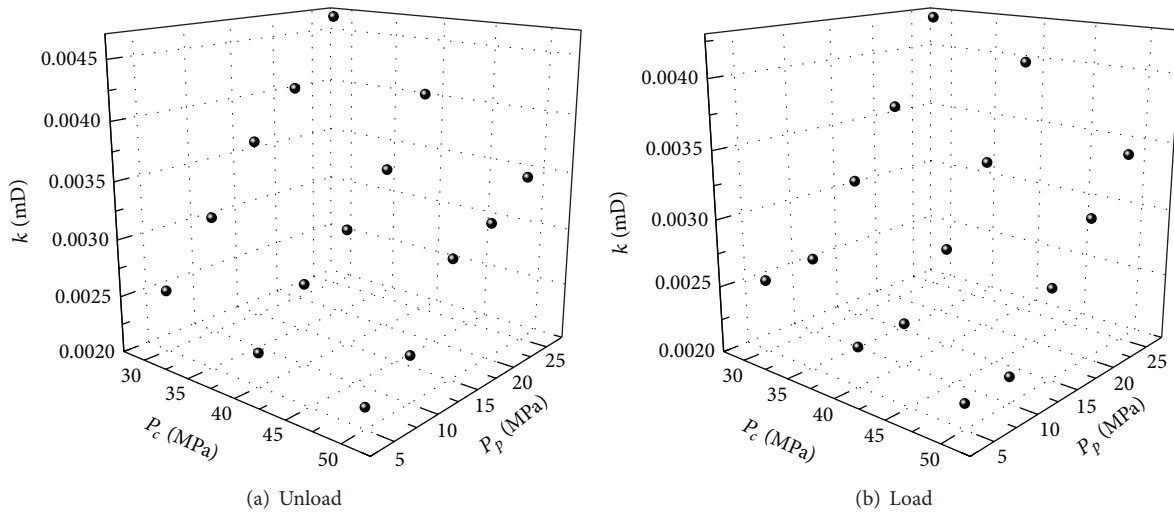


FIGURE 8: Permeability versus pore pressure and confining pressure measured by distilled water when unloading (a)/loading (b) the pore pressure under three different confining pressure conditions.

(2) When measured by distilled water, the sample ESCK is larger than that measured by nitrogen or brine. And the largest ESCK value, 7.01, was measured during pore pressure unloading processes. Furthermore, Nur et al.'s study also measured the ESCK of a sandstone sample with 20% clay, 7.1, to be the largest.

(3) When measured by brine, the sample ESCK is between that measured by nitrogen and distilled water. And the average ESCK values measured under pore pressure unloading and loading conditions are very close, 1.61 and 1.63, respectively. The potassium ion (K^+) of brine partly restrains the expansion of montmorillonite due to its water sensitivity, which to some extent recovers the sample's permeability.

3.4. ESCK Evaluation. From the above experimental results, the ESCK is variable which fails to be consistent with the

traditional conception of ESCK that considered it constant. Hence, an evaluation method was adopted to evaluate the ESCK values measured in this study. Based on permeability stress laws, the effective stress P_{eff} can be equated with $P_{\text{eff}} = P_c - \kappa P_p$. Then the relationship between the effective stress and permeability can be established to be discussed. Therefore, the effective stress versus permeability based on the response surface method ($P_{\text{eff-RSM}} = P_c - \kappa P_p$) studied in this paper can be comparatively analyzed with those on Terzaghi's effective stress law ($P_{\text{eff-T}} = P_c - P_p$). And those relationships of effective stress with permeability with different fluid media, nitrogen, distilled water, and brine are shown in Figures 10~12, respectively.

According to Figures 10, 11, and 12, the relationship of the effective stress on basis of the response surface method with permeability has a better correlation than that on Terzaghi's

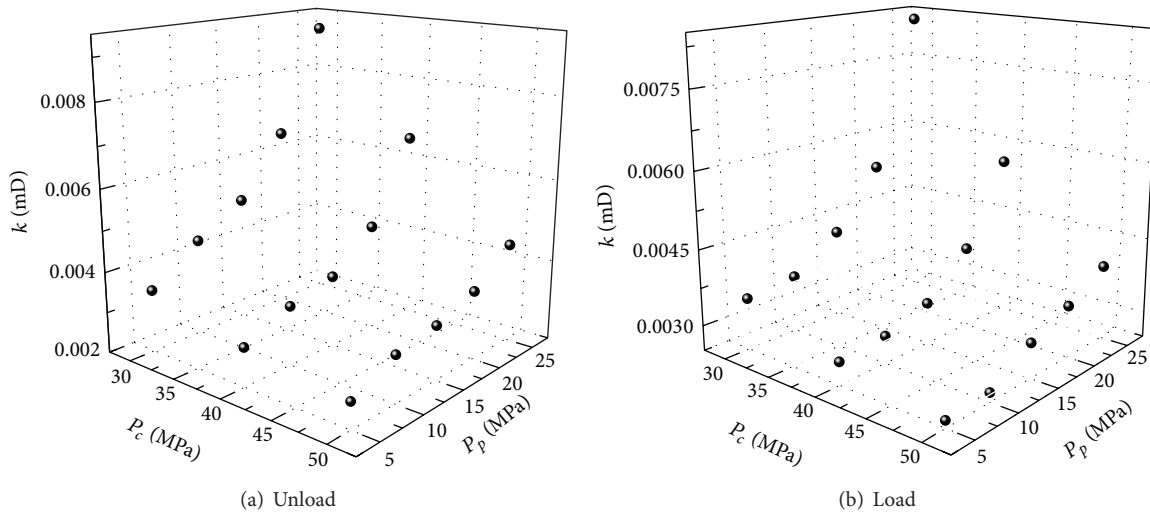


FIGURE 9: Permeability versus pore pressure and confining pressure measured by brine when unloading (a)/loading (b) the pore pressure under three different confining pressure conditions.

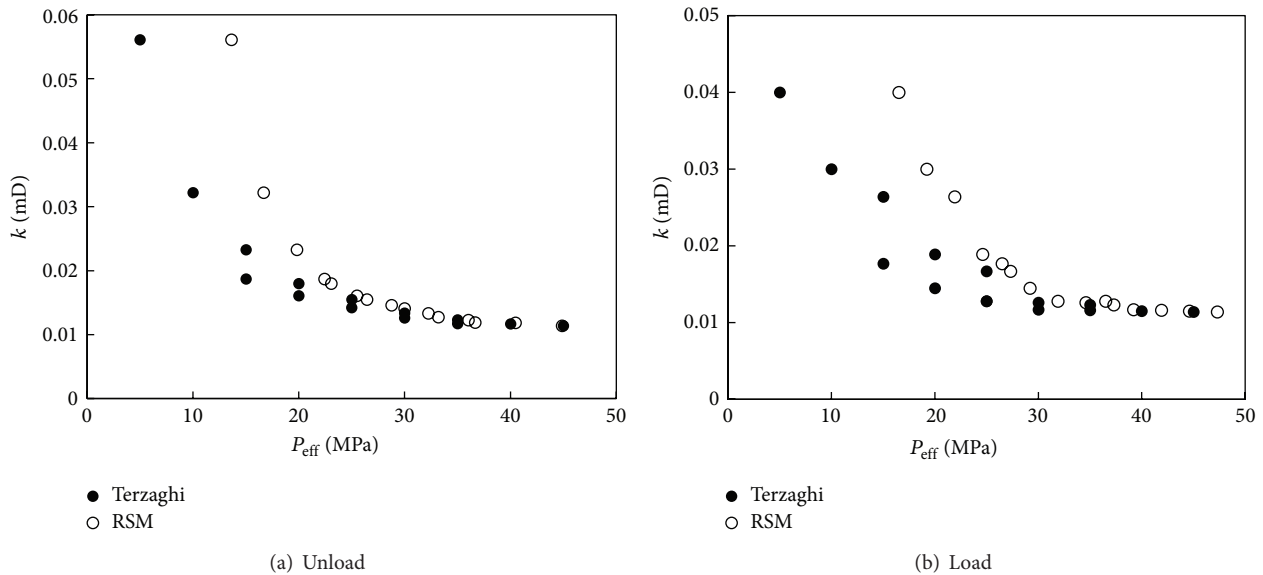


FIGURE 10: Permeability versus effective pressure under nitrogen condition during pore pressure unloading (a)/loading (b) processes.

effective stress law and reveals a one-one correspondence. In addition, referring to the conception of effective stress, that is, the permeability under the same effective stress condition being always the same, it is reasonably concluded that those relationships of effective stress based on the response surface method with the corresponding permeability accord with the conception of effective stress. Hence, the ESCK calculated in accordance with the response surface method is available.

3.5. Discussion. In this study, all of rock permeabilities were measured under the same external experimental conditions, including temperature and loading/unloading confining pressure/pore pressure processes. Therefore, those permeabilities, corresponding to the same effective stress, display differently due to different fluid media only.

(1) The elastic moduli of rock matrix and clay minerals impact rock ESCK. The greater the elastic modulus of clay minerals is different with that of rock matrix, the larger the rock ESCK is. According to previous studies on the elastic modulus of clay minerals, the elastic modulus of kaolinite is between 1.5 and 56 GPa [15–18], of montmorillonite is 6~29.7 GPa [15, 18], and of illite-montmorillonite interlayer ($\phi = 0$, ratio of illite and montmorillonite is 0.6) is 36.7 GPa [18]. Besides, the elastic modulus of dry clay minerals is close to that of quartz [18]. But the elastic modulus of clay minerals, which encounters with water and attaches water-layer to their surfaces, will largely decrease. The relationship of the elastic modulus of Longyou Grottoes sandstone with the water content studied by Shao et al. [19] demonstrated that the elastic modulus decreases exponentially with increasing

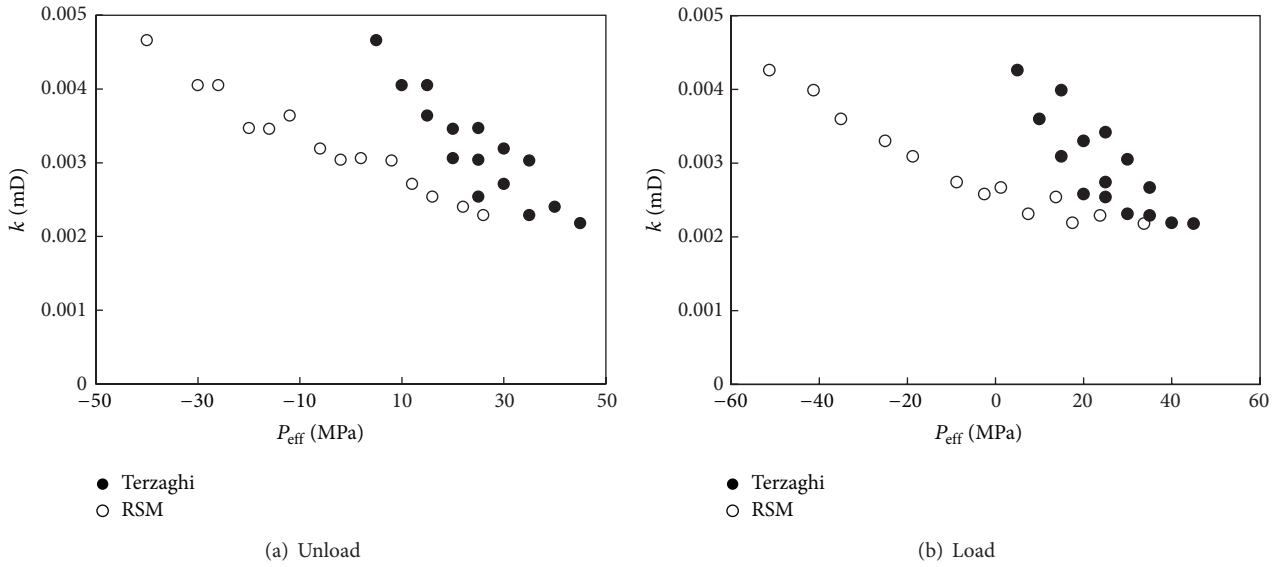


FIGURE 11: Permeability versus effective pressure under distilled water condition during pore pressure unloading (a)/loading (b) processes.

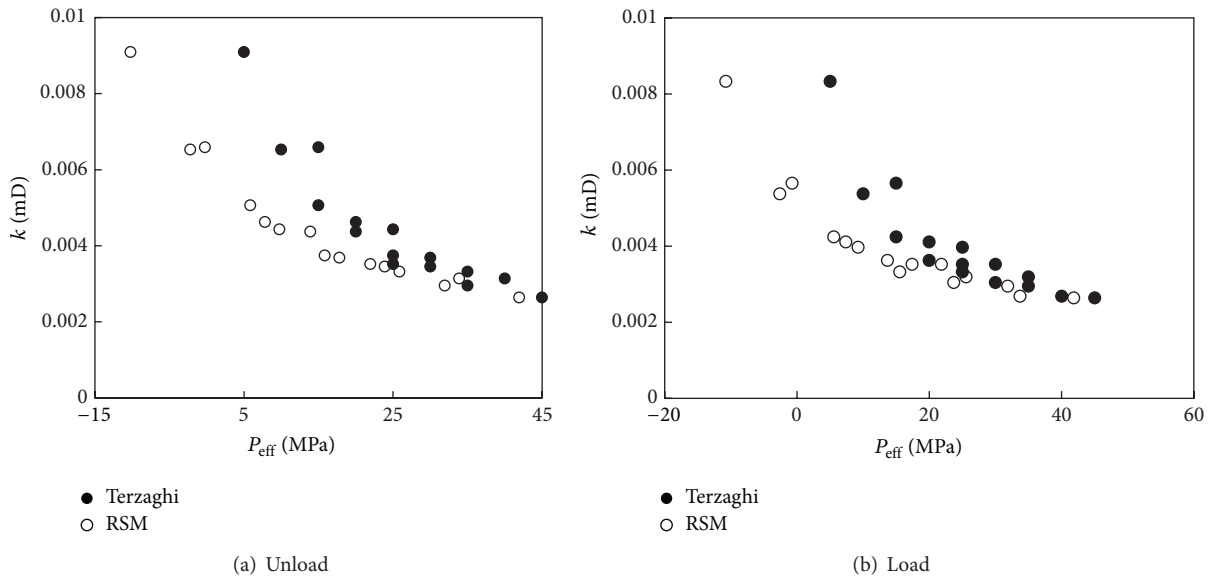


FIGURE 12: Permeability versus effective pressure under brine condition during pore pressure unloading (a)/loading (b) processes.

TABLE 2: Conversion factors and regression coefficients measuring by nitrogen, distilled water, and brine.

Sample	Media	Pore pressure	λ	Regression coefficients					
				a_1	a_2	a_3	a_4	a_5	a_6
HH 50-06	Nitrogen	Unload	-1.904	1972	-163.8	99.78	1.325	-1.271	0.2864
		Load	-2.051	9044	-527.2	104.6	5.002	-2.457	2.447
	Distilled water	Unload	-0.106	-7.492	-0.056	0.091	$5.29E - 04$	$-4.56E - 04$	$-7.26E - 04$
		Load	-0.934	-188.4	-4.923	1.948	0.0330	0.0194	0.1198
	Brine	Unload	-1.155	-177.1	-20.69	22.89	0.1256	-0.1032	0.0117
		Load	-1.594	9520	-263.1	16.81	1.483	0.5965	5.655

TABLE 3: Results of ESCK measured by three different fluid media.

Sample	Fluid media	Pore pressure	Range	Average value
HH50-06	Nitrogen	Unload	(0.65, 1.04)	0.78 ± 0.11
		Load	(0.16, 1.18)	0.54 ± 0.30
	Distilled water	Unload	(1.13, 7.01)	2.80 ± 1.69
		Load	(1.31, 6.25)	3.25 ± 1.39
	Brine	Unload	(1.30, 2.06)	1.61 ± 0.24
		Load	(0.53, 3.30)	1.63 ± 0.79

of water content. Therefore, changing of pore pressure can be more easily causing change of permeability than that of confining pressure due to the decreasing of elastic modulus, which also can show why the ESCK measured by distilled water is the largest.

(2) Swell of clay due to water affects the rock ESCK. When the montmorillonite meets with water, the water can go into interlayers so as to swell the mineral crystals. And the crystal lattice has some extensibility and dispersibility. Different kinds of clay particles can absorb different number of water molecules and form different sizes and numbers of gel groups. As a result, the variation of rock permeability is different. From Zhao's study [20] of various kinds of clay minerals, the permeability measured by aqueous media decreases the most caused by montmorillonite, and the permeability decreases half the range due to kaolinite or illite. Moreover, the rock matrix is relatively loose so that the rock swells and likely spalls. Thus, the pore channels of rock can be possibly blocked so as to reduce its permeability. However, there are only 19.6% mixed-layer minerals of illite and montmorillonite in the measured sandstone sample; its permeability measured by distilled water is just 10% of that measured by nitrogen with the same effective stress condition. This proves that the clay minerals cause large decline of permeability and the ESCK is the largest with distilled water as the fluid medium.

(3) Brine softens the effect of water on the rock ESCK. Because of suppressing the expansion of the clay minerals by saline ions (e.g., potassium ion, K^+), the permeability measured by brine is about 20% of that measured by nitrogen so that the corresponding ESCK is less than that measured by distilled water.

4. Conclusions

- (1) The ESCK values of fine sandstone were measured by three different fluid media, nitrogen, brine, and distilled water, based on the response surface method. As a result, the ESCK is the smallest with nitrogen, the largest, 7.01, with distilled water, and the middle with brine.
- (2) According to the one-one correspondence of effective stress and permeability, the ESCK values studied in this paper were approved to be valid.
- (3) The elastic modulus of clay minerals decreases when the water comes into contact with clay minerals and the clay swells and spalls some particles to block pore throats.

- (4) Compared with distilled water, brine, mainly the saline ions like K^+ , softens water sensitivity impacts on clay minerals. The ESCK values of one sample measured by different fluid media with the same effective stress are different. However, the gas like nitrogen is affected a little by the microscopic characteristics of rock sample. Hence, the reliability of the ESCK measurement is depending on the properties of rock or reservoir itself. For instance, nitrogen or gas is the best fluid medium for measuring the ESCK of gas reservoir and brine is the best for measuring oil reservoir.

Conflict of Interests

The authors declare that there is no conflict of interests regarding the publication of this paper.

Acknowledgments

This research is financially supported by National Natural Science Foundation of China under Grant no. 41274114 and by University-Wide Scientific and Technological Foundation of SWPU under Grant no. 2013XJ2003.

References

- [1] M. Li and W. Xiao, "Experimental study on permeability-effective-stress law in low-permeability sandstone reservoir," *Chinese Journal of Rock Mechanics and Engineering*, vol. 27, no. 2, pp. 3535–3540, 2008.
- [2] K. Terzaghi, "The shearing resistance of saturated soils and the angle between the planes of shear," in *Proceedings of the 1st International Conference on Soil Mechanics and Foundation Engineering*, vol. 1, pp. 54–56, Cambridge, Mass, USA, June 1936.
- [3] N. R. Warpinski and L. W. Teufel, "Determination of the effective stress law for permeability and deformation in low-permeability rocks," *SPEFE*, vol. 7, no. 2, pp. 123–131, 1992.
- [4] A. M. Nur, J. D. Walls, K. Winkler et al., "Effects of fluid saturation on waves in porous rock and relations to hydraulic permeability," *Society of Petroleum Engineers Journal*, vol. 20, no. 6, pp. 450–458, 1980.
- [5] C. A. Morrow, Z. Bo-Chong, and J. D. Byerlee, "Effective pressure law for permeability of westerly granite under cyclic loading," *Journal of Geophysical Research*, vol. 91, no. 3, pp. 3870–3876, 1986.

- [6] Y. Bernabe, "The effective pressure law for permeability during pore pressure and confining pressure cycling of several crystalline rocks," *Journal of Geophysical Research*, vol. 92, no. 1, pp. 649–657, 1987.
- [7] K. B. Coyner, *Effects of Stress, Pore Pressure and Pore Fluid on Bulk Strain, Velocity, and Permeability in Rocks*, Massachusetts Institute of Technology, Cambridge, Mass, USA, 1984.
- [8] O. Kwon, A. K. Kronenberg, A. F. Gangi, and B. Johnson, "Permeability of Wilcox shale and its effective pressure law," *Journal of Geophysical Research B: Solid Earth*, vol. 106, no. 9, pp. 19339–19353, 2001.
- [9] W. Al-Wardy and R. W. Zimmerman, "Effective stress law for the permeability of clay-rich sandstones," *Journal of Geophysical Research B: Solid Earth*, vol. 109, no. 4, Article ID B04203, 2004.
- [10] G. Boitnott, T. Miller, and J. Shafer, "Pore pressure effects and permeability: effective stress issues for high pressure reservoirs," in *Proceedings of the International Symposium of the Society of Core Analysts (SCA '09)*, p. 9, Noordwijk, The Netherlands, September 2009.
- [11] M. D. Zoback and J. D. Byerlee, "Permeability and effective stress: geologic notes," *AAPG Bulletin*, vol. 59, no. 1, pp. 154–158, 1975.
- [12] R. L. Kranz, A. D. Frankel, T. Engelder, and C. H. Scholz, "The permeability of whole and jointed Barre Granite," *International Journal of Rock Mechanics and Mining Sciences & Geomechanics Abstracts*, vol. 16, no. 4, pp. 225–234, 1979.
- [13] S. C. Jones, "A technique for faster pulse-decay permeability measurements in tight rocks," *SPE Formation Evaluation*, vol. 12, no. 1, pp. 19–24, 1997.
- [14] W. F. Brace, J. B. Walsh, and W. T. Frangos, "Permeability of granite under high pressure," *Journal of Geophysical Research*, vol. 73, no. 6, pp. 2225–2236, 1968.
- [15] K. W. Katahara, "Clay mineral elastic properties," in *Proceedings of the SEG Annual Meeting Expanded Technical Programme Abstracts*, Paper RP1.4, pp. 1691–1694, 1996.
- [16] A. F. Woeber, S. Katz, and T. J. Ahrens, "Elasticity of selected rocks and minerals," *Geophysics*, vol. 28, no. 4, pp. 658–663, 1963.
- [17] T. Vanorio, M. Prasad, and A. Nur, "Elastic properties of dry clay mineral aggregates, suspensions and sandstones," *Geophysical Journal International*, vol. 155, no. 1, pp. 319–326, 2003.
- [18] Z. Wang, H. Wang, and M. E. Cates, "Effective elastic properties of solid clays," *Geophysics*, vol. 66, no. 2, pp. 428–440, 2001.
- [19] M. Shao, L. Li, and Z. Li, "Elastic wave velocity and mechanical properties of sandstone under different water contents at Longyou grottoes," *Chinese Journal of Rock Mechanics and Engineering*, vol. 29, no. 2, pp. 3514–3518, 2010.
- [20] G.-W. Zhao, H.-H. Fan, H. Chen, and M. Shi, "Influence of montmorillonite on dispersivity of clayey soils," *Chinese Journal of Geotechnical Engineering*, vol. 35, no. 10, pp. 1928–1932, 2013.



Hindawi

Submit your manuscripts at
<http://www.hindawi.com>

